Solid-State NMR Investigation of Paramagnetic Nylon-6 Clay Nanocomposites. 2. Measurement of Clay Dispersion, Crystal Stratification, and Stability of Organic Modifiers

D. L. VanderHart,*,† A. Asano,‡ and J. W. Gilman§

National Institute of Standards and Technology, Gaithersburg, Maryland 20899-8544

Received February 13, 2001. Revised Manuscript Received August 16, 2001

In this second paper of a two-part series dealing mainly with NMR characterization of nylon-6/clay nanocomposites (NnC's) having nominally 5 mass % clay, measurements with application to processing are featured. The paramagnetism of the montmorillonite clays, discussed in the first paper, allowed us to use the corresponding spin-diffusion-moderated reduction in longitudinal proton relaxation time, T_1^H, for two purposes, namely, to rank the quality of clay dispersion in NnC families with the same formulation and to investigate morphological stratification of the nylon-6 α- and γ-crystallites with respect to the clay surface. In a group of three NnC's with the same formulation but different melt-blending conditions, variations in T_1^H correlated well with previously published TEM assessments of the quality of the clay dispersion. Also, in a set of samples from an injection-molded, in situ polymerized NnC disk where strong variations in α/γ ratios were observed, it was found that these differences did not arise from processing-induced inhomogeneities in clay concentration; rather, variations in cooling histories throughout the disk was the more probable cause. In these latter samples, well-defined stratification of the γ-phase (versus the α-phase) crystallites nearer the clay surface did not occur until after annealing at 214 °C. We also examined the dependence of NnC T_1^H's on the static field of the measurement. It is clear that the magnitude of the paramagnetic contribution to T_1^H is a function of field and of Fe^{3+} concentration in the clay. Trends support the notion that spin-exchange interactions between the electrons on different Fe^{3+} ions largely define the spectral density of magnetic fluctuations near the clay surface. Some attention was, therefore, given to optimizing Fe^{3+} concentrations for the best NnC characterization. Finally, we investigated the chemical stability of a particular organic modifier (OM), which is used to pretreat the clay prior to melt blending. The OM, dimethyl, dehydrogenated-tallow ammonium ion, was followed in the process of blending this modified clay with nylon-6 at 240 °C. It was found that when such a clay surface was exposed to the nylon-6 during blending, most of the OM on that surface decomposed, releasing a free amine with one methyl and two tallow substituents. However, subsequent melting at 240 °C produced no further decomposition. The implication is that the *combination* of temperature and shear stress in blending causes decomposition, not just temperature alone. The susceptibility to chemical decomposition varied strongly with the OM. Ironically, extensive decomposition of the OM did not result in poor mixing; in fact, as judged by T_1^H, the NnC with the best dispersion of clay also had the most extensively degraded OM. The implications of this degradation for the physical properties have not been explored in detail.

Introduction

In the first part of this two-part series, we reported[1] studies of exfoliated nylon-6/clay nanocomposites (NnC's), with nominally 5 mass % clay. Both in situ polymerized (IsP) and blended NnC's were represented. On the basis of DSC data, qualitative trends were deduced relating to the crystallization of nylon-6 in the presence of clay platelets. We also reported NMR findings concerning the clay-dependent initiation of γ-phase crystallization, the stability of this γ-phase in the presence of annealing at 214 °C, and the morphological and dynamic similarity of both pure nylon-6 and the NnC's when each is prepared by melt crystallization at a cooling rate of 1 °C/min or subsequently subjected to annealing.

The final topic of the first paper dealt with paramagnetic Fe^{3+} that is embedded in the 1-nm-thick clay layers.[2] The unpaired electrons ($S = 5/2$) on this nucleus produce a major perturbation on protons and ^{13}C nuclei within about 1 nm of the clay surface. As an indication

* To whom correspondence should be addressed.
† Polymers Division.
‡ Polymers Division. Current address is Department of Applied Chemistry, National Defense Academy, 1-10-20 Hashirimizu, Yokosuka 239-8686, Japan.
§ Fire Science Division.

(1) VanderHart, D. L.; Asano, A.; Gilman, J. W. *Chem. Mater.* 2001, *13,* 3781.

10.1021/cm011078x
Published on Web 09/27/2001

of the importance of this perturbation for nuclei within 0.4 nm of a clay surface, NMR measurements were reported[1] for the ^{13}C and proton nuclei belonging to the organic modifier (OM) that is applied to the clay to facilitate a good dispersion of clay particles throughout the nylon-6 matrix. In these organically modified clays (OMCs) the Fe^{3+} causes significant line broadening, partial signal loss, and a substantial shortening of both the longitudinal and the rotating frame nuclear relaxation times. From these observations, the magnetic fluctuations associated with the paramagnetic Fe^{3+} sites were deduced to have significant spectral densities in both the MHz and the mid-kHz regions.

In this paper we deal with topics that are more relevant to processing of NnC's. In particular, we first propose a relative assay for the quality of the clay dispersion for families of similarly formulated NnC's when paramagnetic montmorillonite clays are employed. Because mechanical-property enhancements typify these NnC's,[3] the quality of the clay dispersion is important to correlate with mechanical properties. In assessing the quality of the dispersion, we make use of the favorable spectral density in the MHz region associated with the Fe^{3+} impurity sites embedded in the montmorillonite-clay layers. In the first paper of this series,[1] we have seen that the protons within about 0.4 nm of the clay surface will have notably shorter T_1^H values than what would pertain in the absence of the Fe^{3+} ions. If we further consider the phenomenon of proton spin diffusion,[4] we have a mechanism for propagating this enhanced relaxation to protons much more distant from the clay surfaces. As will be seen, T_1^H at 100 MHz for nylon-6 protons in the absence of clay is about 0.5 s, and within that 0.5-s time frame, all he protons within a distance of about 25 nm from a clay surface could experience, via spin diffusion, a noticeable decrease in T_1^H. (This 25-nm distance is computed to be the rms distance, X, that polarization can travel in a time, $t = 0.5$ s, using the one-dimensional diffusion equation[5]

$$X = (2Dt)^{1/2} \quad (1)$$

where we assume a proton spin diffusion constant, D, of 0.7 nm^2/ms for nylon-6[6,7] and, for simplicity, a proton polarization at the clay surface that, owing to efficient paramagnetic relaxation, remains close to the Boltzmann level.)

Recognizing that TEM micrographs of these NnC's generally show that poor exfoliation results in some clay platelets that are not separated, it follows that the best clay dispersions will also have the shortest average distance between polymer/clay interfaces. Hence, considering that the paramagnetic contribution to T_1^H propagates away from the clay surface in a diffusive manner, the average paramagnetic contribution to T_1^H will be greater for smaller average distances between polymer/clay interfaces. For families of NnC's with the same clays (i.e., the same Fe^{3+} concentrations in each clay layer) and the same nylon-6/clay stoichiometry, T_1^H is expected to be correlated with the quality of clay dispersion. In this paper, we will demonstrate this point. Also, we will report on T_1^H measurements in a multiply sampled, injection-molded disk that exhibited substantial variations in the ratio of crystallites having the α- or γ-form. These T_1^H measurements are used to test the hypothesis that injection molding induces macroscopic inhomogeneities in the concentration of clay.

A corollary is that the closer to the clay surface that a spin is, the stronger will be the paramagnetic influence on T_1^H. Hence, there is also the opportunity to investigate the spatial stratification of any components that can be spectrally identified. A case considered herein is the relative stratification of the α-form[8] and the γ-form[9,10] crystallites when representative amounts of each are present in a single sample. To the extent that the mechanical properties of the two crystal forms are different, the details of mixing of the two forms may have implications for mechanical properties.

The final major topic we treat in this paper relates to the chemical stability of the organic modifier (OM) through the processing stage where polymer/clay melt-blending occurs. This is not a systematic study. Rather, we document extensive degradation in one type of OM, given that fortuitous circumstances allow us to identify and quantify the degradation products. Preliminary data suggest that there is a wide variation in the extent of degradation for different OM's; however, this conclusion is based on certain assumptions that remain to be verified. A condensed report of some of these findings has already appeared;[11] this is an amplified report, both in topics and detail.

Experimental Section

Samples. Samples of NnC's are largely described in the first paper[1] of this series and we use the same nomenclature in this paper. Abbreviations used in the sample designations include the following: nylon-6 (N6), nylon-6/clay nanocomposite (N6C), in situ polymerized (Is), blended (B), paramagnetic montmorillonite clay (M), diamagnetic Laponite clay (L), a numerical designation (1, 2, 3 ...) referring to different organic modifiers (OM) used to treat the clays, and finally, a letter suffix that distinguishes samples with different thermal histories. Detailed sample information is included in Table 1. The thermal histories for each sample are ordered chronologically. Aside from the injection molding (IM) history of several of the N6C-Is-M-*x* samples (mold temperature of 80 °C; injector temperature of 295 °C), we commonly melt-crystallized our samples, starting at a melt temperature near 250 °C and cooling at a rate of 1 °C/min (we refer to this melt-crystallization history as "slowly cooled" or "SC"). Annealing (A) was always at 214 °C and the duration was 18 h unless otherwise noted.

(2) *Dana's New Mineralogy*; Gaines, R. V., Skinner, H. C. W., Foord, E. E., Mason, B., Rosenzweig, A., Eds.; John Wiley and Sons: New York, 1997; pp 1480f.

(3) Kojima, Y.; Usuki, A.; Kawasumi, M.; Okada, A.; Fukushima, Y.; Kurauchi, T.; Kamigaito, O. *J. Mater. Res.* **1993**, *8*, 1185.

(4) Abragam, A. *The Principles of Nuclear Magnetism*; Oxford University Press: London, 1961; Chapter V.

(5) Crank, J. *The Mathematics of Diffusion*; Oxford University Press: London, 1957.

(6) Clauss, J.; Schmidt-Rohr, K.; Spiess, H. W. *Acta Polym.* **1993**, *1*, 44.

(7) VanderHart, D. L.; McFadden, G. B. *Solid State Nucl. Magn. Reson.* **1996**, *7*, 45.

(8) Holmes, D. R.; Bunn, C. W.; Smith, D. J. *J. Polym. Sci.* **1955**, *17*, 159.

(9) Arimoto, H.; Ishibashi, M.; Hirai, M. *J. Polym. Sci. (A)* **1965**, *3*, 317.

(10) Bradbury, E. M.; Brown, L.; Elliott, A.; Parry, D. A. D. *Polymer* **1965**, *6*, 465.

(11) VanderHart, D. L.; Asano, A.; Gilman, J. W. *Macromolecules* **2001**, *34*, 3819.

Table 1. Sample Information for Nylon-6/Clay Nanocomposites Having Nominally 5 mass % Clay: Thermal Histories, Paramagnetism (Paramag), Type of Organic Modifier, NMR-Determined Fraction of Crystalline Material that is α-phase (f_α), and Proton Longitudinal Relaxation Times, (T_1^H) for Materials Subjected to Different Thermal Histories

					T_1^H [e] (ms)	
sample[a]	thermal history[b]	Paramag?	organic modifier[c]	f_α[d]	2.35 T	7.05 T
N6-a	SC	N	none	1.00	529	1625
N6-b	SC/A	N		1.00	592	1645
N6C-Is-M-a	IM	Y	12-aminolauric acid	0.10 to 0.45	327	708
N6C-Is-M-c	IM/A	Y		0.42−0.75*	366	800
N6C-Is-M-d	IM/SC	Y		0.10*		
N6C-Is-M-e	IM/SC/A	Y		0.63*		
N6C-Is-M-f	SC	Y		<0.04		
N6C-Is-M-g	SC/A(2.5 h)	Y		<0.07		
N6C-Is-M-h	SC/A	Y		<0.12		
N6C-B-L1-b	SC	N	$MT(HE)_2AI$ (0.95)	<0.05	521	1438
N6C-B-L1-c	SC/A(2.5 h)[f]	N		0.13	550	1519
N6C-B-M1-b	SC	Y		<0.02	357	710
N6C-B-M1-c	SC/A(2.5 h)	Y		0.14		
N6C-B-M3-a	SC	Y	M_2T_2AI (1.25)	<0.03	421	938
N6C-B-M3-b	SC	Y		<0.05	400	880
N6C-B-M3-c	SC	Y		<0.03	327	599

[a] Sample abbreviations: nylon-6 (N6), nylon-6/clay nanocomposite (N6C), formation of NnC by in situ polymerization (Is) or physical blending (B), montmorillonite clay (M), Laponite clay (L); numbers refer to different OMs and lowercase letters refer to thermal histories. [b] Abbreviations: "A(*x*)" = annealing at 214 °C for 18 h or for a period *x*, if explicitly indicated. Samples were taken out of oven and cooled on the bench after annealing, unless otherwise indicated. "IM" = injection molding at 295 °C into a dye at 80 °C; and "SC" is melt crystallization from the melt at about 250 °C with an oven cooling rate of 1 °C/min. [c] These substances exchange-modify the clay prior to nanocomposite formation. $MT(HE)_2AI$ = methyl, hydrogenated-tallow, bis-2-hydroxyethyl, quaternary ammonium ion and M_2T_2AI is dimethyl, di(hydrogenated-tallow) quaternary ammonium ion. Numbers in parentheses are the number of equivalents of OM per kilogram of clay. The OM is introduced to the clay with chloride counterions. [d] Based on the relative intensities of the 26.3 ppm (α) and the 34 ppm (γ) lines in the "CR" spectra.[1] Standard uncertainties are estimated at ±0.03; if an * symbol appears next to the value, the standard uncertainty is ±0.05. For the N6C-Is-M-(a,c) samples, ranges are given because 10 different samples were investigated and there was wide variation in f_α (see text). [e] Standard uncertainties for T_1^H measurements are ±2.5% of the given value. Values refer to the final slopes of the T_1^H plots. [f] Cooling rate from the annealing temperature for this sample was 1 °C/min.

Table 2. Reported[12] Blending Conditions and Nanocomposite Characteristics (X-ray diffraction, XRD; Transmission Electron Microscopy, TEM, and Mechanical Properties Using ASTM Methods D638 and D256A) for the Variably Blended N6C-B-M3 Samples with a Comparison to Pure Nylon

	sample			
property	N6C-B-M3-a	N6C-B-M3-b	N6C-B-M3-c	pure nylon 6
estimated quality of clay dispersion	medium	medium	good	N/A
twin-screws of extruder intermeshing?	yes	no	no	N/A
relative shear rate in mixing stage	high	high	medium	N/A
extruder mean residence time (s)	117	136	162	N/A
XRD basal spacing (nm)[a]	3.79	3.79	no peak	N/A
relative XRD area under basal-spacing peak	164	277	no peak	N/A
platelets or intercalates per cm^2 on a TEM image at 130 500 magnification	1.5	3.1	4.2	N/A
tensile modulus (Gpa)	3.4	3.6	4.0	2.7
tensile yield strength (Mpa)	69	80	85	64
% elongation (5 cm/min)	50	60	17	40
% elongation (0.5 cm/min)	>200	>200	39	>200
izod impact (J/m)	43	45	44	37

[a] This is the separation between clay layers that are not exfoliated; completely exfoliated clay has no such associated XRD peak.

Three samples that were not described in the first paper of this series are samples N6C-B-M3-(a, b, and c); some discussion of these samples was included in our previously published communication.[11] These three blended NnC's have the same clay type and nylon-6/clay stoichiometry; only processing conditions were changed. The samples were generated at Southern Clay Products of Gonzales, TX, and were a subset of samples included in a study[12] where mixing conditions were varied and resulting changes in properties and clay dispersions were tracked. Variations included different twin-screw-extruder designs, different shear rates during blending, and different residence times in the extruder. Mixing in these samples was carried out at 240 °C using a Leistritz 34-mm counter-rotating twin-screw extruder, having either inter-meshing or non-inter-meshing character. Table 2 summarizes selected conditions and observations reported[12] for these three samples. These samples qualitatively represent different levels of dispersion of the clay in the NnC, that is, two medium- and one well-dispersed, according to TEM images and X-ray diffraction. These three samples play a major role in the studies where we correlate T_1^H with the quality of clay dispersion and where we follow the degradation of the OM.

NMR Measurements. Two NMR spectrometers were employed, one noncommercial that operates at 2.35 T (100 MHz for protons) and is dedicated to ^{13}C observation with magic-angle sample spinning (MAS). The other spectrometer is a Bruker Avance[13] operating at 7.05 T (300 MHz for protons). Details of operation for the two spectrometers are found in the first paper of this series.

For the T_1^H measurements, the inversion recovery sequence[14] was employed and detection was either indirect via cross-polarization to the ^{13}C nuclei or it was direct, using

(12) Dennis, H. R.; Hunter D. L.; Chang, D.; Kim, S.; White, J. L.; Cho, J. W.; Paul, D. P. Proceedings of *ANTEC 2000*, Orlando, May 2000.

(13) Certain commercial companies are named in order to specify adequately the experimental procedure. This in no way implies an endorsement or recommendation by the authors or their agencies.

Fourier-transformed Bloch-decay proton spectra. In all cases where the α-phase and γ-phase CR signals had to be monitored separately, indirect detection was employed. T_1^H data taken at the two different fields for the same samples allows some insight into the correlation time, τ_e, characterizing the magnetic fluctuations associated with the unpaired Fe^{3+} electrons as sensed by the nuclei near the clay surfaces. We adopt an operational definition for τ_e that includes fluctuations arising from the electron longitudinal relaxation time, T_1^e, as well as the effects of spin exchange[15] between dipolar-coupled electrons on different Fe^{3+} sites.

Error Estimates. Errors given for all quantities that we measured are standard error estimates unless otherwise indicated.

Results

T_1^H's of the Nanocomposites. In Table 1, selected T_1^H's at 100 MHz and a few at 300 MHz are listed for several *dried* nylon-6/clay samples. We found that absorbed water reduces T_1^H; hence, only T_1^H's for dried samples are comparatively meaningful. At 2.35 T, the pure nylon-6 sample, N6, and the N6C-B-L1-b and N6C-B-L1-c samples have T_1^H's in the 520−590-ms range. All the montmorillonite-containing NnC's for which T_1^H's were measured had significantly shorter T_1^H's, thereby indicating that the paramagnetic contribution to the T_1^H's is not negligible. Moreover, the fact that the T_1^H's of N6 and the N6C-B-L1 samples with comparable thermal histories differ by <10% suggests that there is no significant change in the average high-frequency motions in the NC regions of nylon, which results from the presence of the clay.

It is expected that, in the pure nylon, the protons in the NC region will be more mobile and have significantly shorter intrinsic T_1^H's than will the protons in the CR region. At 2.35 T, for example, in annealed nylon-6, the ^{13}C longitudinal relaxation time, T_1^C, for methylene protons is, on average, <300 ms in the NC region and >65 s in the CR region; this is a >200-fold difference. The intrinsic T_1^H's would be expected to be of the same order and possess a similar disparity. Hence, protons in the CR region will relax mainly by spin diffusion from the NC region. It follows that the final slope in a semilogarithmic T_1^H plot is determined not only by the intrinsic T_1^H's of the CR and NC regions but also by the crystallite thickness and the crystalline fraction, f_c. According to Table 1, annealing will generally increase T_1^H by a modest amount, even though the corresponding NMR crystallinity, within experimental error, does not increase significantly over that of SC samples.

T_1^H behavior for the paramagnetic NnC's is more complicated. At clay loadings characteristic of the samples studied herein, one expects that if the clay is uniformly exfoliated, there will be a mean separation of about 40−70 nm between clay platelets. This distance is larger than the 16-nm-long spacing[1] of the semicrystalline morphology. Hence, the paramagnetic contribution to relaxation, which originates from the clay platelets and propagates through the nylon-6 by spin diffusion, is not expected to influence each region to the same degree. Those regions, including crystallites, which are closest to the surface of the clay will be influenced most strongly. We will use this idea in the next section when T_1^H data allow us to inquire whether the γ-crystallites are closer to the surface of the clay than are the α-crystallites. In the absence of paramagnetic contributions, the final slope in a T_1^H plot for all protons is expected to be achieved in a time comparable to the spin equilibration time (16−20 ms)[1] between CR and NC regions. After such a time, a steady-state polarization gradient is established and the whole system appears to relax with a single time constant. In the presence of the paramagnetic clay, those nuclei that are most isolated from the clay (in the mid-plane between two clay surfaces) will have T_1^H decays, which achieve a limiting slope in a time of about 300 ms for a 40-nm separation and about 900 ms for a 70-nm separation. These times are characteristic of spin diffusion over a distance of half the average separation between clay layers (spin diffusion propagates from both clay surfaces).

We can try to isolate the paramagnetic contribution to T_1^H using the approximate "sum-of-rates" equation

$$(T_{1para}{}^H)^{-1} = (T_1{}^H)^{-1} - [(T_1{}^H)_{N6}]^{-1}, \qquad (2)$$

where $T_{1para}{}^H$ is the paramagnetic contribution and $(T_1^H)_{N6}$ is the T_1^H for pure nylon-6. Besides producing an accelerated average decay rate, another important characteristic of the paramagnetic contribution to T_1^H is a more accelerated decay with nonexponential character at shorter times. The magnitude of this nonexponential contribution is dependent on position from the clay surface; the closer is the spin to the surface, the larger this contribution. However, after some time, a steady-state spin-polarization gradient develops and all spins appear to decay with the same time constant. We use the convention that T_1^H in eq 2 is measured over those times after which this steady-state has been achieved. Thus, the approximate character of eq 2 arises from the fact that this relationship ignores the position-dependent nonexponential character of the initial decay. It turns out that $T_{1para}{}^H$, as expresssed in eq 2, will depend on the average separation between clay layers as well as the efficiency of direct paramagnetically induced proton relaxation near the clay surfaces. Nevertheless, eq 2 is a useful relationship because $T_{1para}{}^H$ will be more sensitive to the quality of clay dispersion than will T_1^H. Moreover, by comparing $T_{1para}{}^H$ values for the same sample at different magnetic fields, one can gain some insight into the dependence of τ_e on the static field for different types of clay. If $T_{1para}{}^H$ values are the same in two different static fields for the same sample, then one can conclude that the relevant spectral densities, associated with τ_e, at the two Larmor frequencies are the same. That, in turn, implies that $\tau_e \ll \omega_L{}^{-1}$ where ω_L is the Larmor frequency in rad/s. On the other hand, when $\tau_e > \omega_L{}^{-1}$, $T_{1para}{}^H$ will be shorter at the lower field. Because $T_{1para}{}^H$ involves a diffusive propagation of relaxation and because one is neither in the diffusion-controlled nor the relaxation-controlled regime in the systems we are dealing with, the dependence of $T_{1para}{}^H$ on the inverse spectral density at the Larmor frequency is neither linear nor quadratic. In other words, the ratio of the $T_{1para}{}^H$'s at the two fields

(14) Farrar, T. C.; Becker, E. D. *Pulse and Fourier Transform NMR*; Academic Press: New York, 1971; pp 20f.

(15) Poole, C. P. *Electron Spin Resonance*; Interscience Publishers: New York, 1967.

Table 3. Paramagnetic Contributions[a] to T_1^H Using Equation 2 for Several Nanocomposites and Different Static Fields

	T_{1para}^H (ms)	
sample	2.35 T	7.05 T
N6C-Is-M-c's (ave)	960(80)	1560(90)
N6C-B-M1-b	1100(120)	1260(60)
N6C-B-M3-a	2060(380)	2220(160)
N6C-B-M3-b	1640(230)	1920(130)
N6C-B-M3-c	860(70)	950(40)

[a] Based on eq 2 where the nylon-6 reference T_1^H relates to a sample with a corresponding thermal history. Standard uncertainties are indicated in parentheses in units of the least significant figure.

will be closer to unity than the corresponding inverse ratio of spectral densities at the two Larmor frequencies.

In Table 3 we list T_{1para}^H values for samples N6C-Is-M-c (average values), N6C-B-M1-b, and N6C-B-M3-(a,b,c). The latter three samples are alike in all respects except for the blending conditions and all are SC samples except for N6C-Is-M-c (annealed). The relative ranking of the quality of clay dispersion implied by T_{1para}^H (and T_1^H) fully agrees with the TEM analysis of Table 2 for the N6C-B-M3 samples. In contrast to the considerably different T_1^H values in Table 1 at the two fields for a given sample, the T_{1para}^H values for all but the N6C-Is-M-c samples overlap, within experimental error. Because $(T_{1para}^H)^{-1}$ values for the same sample at different magnetic fields are related to the spectral density of the electron fluctuations at each respective proton Larmor frequency, ω_L, the nearly field-independent T_{1para}^H's for all but the N6C-Is-M-c samples suggest that τ_e for this particular clay is comparable to or less than $[(\omega_L(7.05\ T)]^{-1} = 5 \times 10^{-10}$ s. In contrast to this, the dependence of T_{1para}^H on field for the N6C-Is-M-c samples suggests that $\tau_e > 5 \times 10^{-10}$ s for that clay. That both the foregoing relationships should characterize τ_e in different clays is consistent with the suggestion[16] that the τ_e values are largely determined, not by intrinsic longitudinal relaxation rates for the isolated Fe^{3+} ion, but by spin exchange interactions between Fe^{3+} sites. Such exchange rates increase as the average distance between Fe sites decreases; hence, we conclude that the Fe^{3+} concentration in the clay used in the IsP NnC is lower than that in the clay used in the blended NnC's.

If we compare the T_{1para}^H values for N6C-Is-M-c and N6C-B-M3-c, the values are comparable at 2.35 T but are quite different at 7.05 T. They are comparable at 2.35 T because there is approximately a 50% greater mass fraction of clay in the former NnC and this effect is offset by the smaller spectral density at ω_L. At 7.05 T, the values diverge, reflecting the significant loss of spectral density at ω_L for the N6C-Is-M-c sample. Among the four blended NnC's in Table 3, the ordering of the T_{1para}^H values would rank the N6C-B-M1-b sample as having the second best dispersion, given that the clays used are the same and the nylon-6/clay stoichiometries are very similar.

We emphasize that the T_{1para}^H measurement, when used to compare the relative quality of clay dispersion, will be subject to uncertainties that arise if one cannot accurately control the clay/polymer stoichiometry or if one expects substantial variation from batch to batch in the Fe^{3+} concentrations of the clay. For an estimate of the fractional change in effective clay concentration associated with a fractional change in T_1^H, see the Discussion section.

We return briefly to the N6C-Is-M-a and -c samples. As previously indicated, several (about 10) NMR samples of N6C-Is-M-a were made and different regions of this single injection-molded disk were sampled. We did this multiple sampling after we realized that the fraction, f_α, of the crystallites in the α form varied over a wide range, from about 0.10 to 0.45. These samples were all subsequently annealed at 214 °C for 18 h whereupon f_α generally increased by 0.2−0.4 with the result that $0.42 < f_\alpha < 0.75$. In addition, f_α showed no simple correlation with position in the injection-molded disk whose mold temperature at the time of injection was 80 °C. The question that we had was whether there might be a variation in the dispersion of clay that would account for the differences in f_α or whether f_α was mainly reporting local differences in cooling rate in a situation where f_α was sensitive to cooling rate. Thus, we measured T_1^H's for dried samples, both before and after annealing to check on the possibility that substantial variations in the concentration of clay were present. Each group of measured T_1^H's, separated according to field and thermal history, deviated from their respective mean values by <3%, a deviation only slightly above the estimated (±2.5%) accuracy of the T_1^H measurements. Hence, *the variation in f_α is mainly not related to variations in clay concentration*, but rather, we believe, to variations in the local cooling rates. However, given that there is also something irreversible, which we do not fully understand,[1] that has happened to these injection-molded samples, such that a larger than normal fraction of the material converts to the α form upon annealing, it is also possible that these variations in f_α reflect something other than cooling rate variations. For example, there might be local variations in the degree of degradation of the OM. We cannot really dismiss this possibility.

Identification of the Type of Crystallites Closer to the Clay Surface. On the basis of the foregoing considerations, one can test if there is any correlation between the kind of crystallite (α or γ) and its average proximity to the clay surface. We expect that if a NnC sample possesses substantial amounts of both α- and γ-crystallites, then, on average, the γ-crystallites will be more proximate to the surfaces of the clay layers than will the α-crystallites. Because the mere presence of the clay is sufficient[17,18] to change the dominant crystal habit from α to γ, it seems a small additional assumption that the γ-phase would be nucleated mainly at the surface of the clay particles, thereby placing these γ-crystallites closer to the clay surfaces.

In most of these NnC samples, the γ-phase is so dominant that one expects the T_1^H of the γ-phase crystallites to approach the sample-average T_1^H. Then,

(16) Yang, D.-K.; Zax, D. B. *J. Chem. Phys.* **1991**, *110*, 5325.

(17) Kojima, Y.; Usuki, A.; Kawasumi, M.; Okada, A.; Kurauchi, T.; Kamigaito, O.; Kaji, K. *J. Polym. Sci. (B) Polym. Phys.* **1994**, *32*, 625.

(18) Maxfield, M.; Christiani, R.; Murthy, S. N.; Tuller, H. U.S. Patent 5,385,776, 1995.

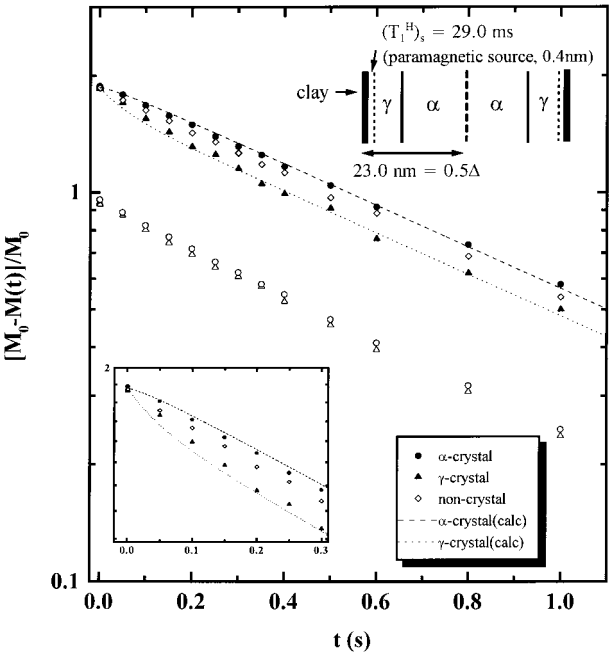

Figure 1. ^{13}C-detected 300-MHz-T_1^H decay curves for a particular N6C-Is-M-a (f_α = 0.45) and its annealed N6C-Is-M-c counterpart (f_α = 0.75). The figure legend identifies components in the decay of the latter sample. Vertically offset decays for the unannealed N6C-Is-M-a sample utilize open symbols, which replace the previously closed symbols. The simplified computational model used to generate the fits to the N6C-Is-M-c decays for the α-crystal and γ-crystal is shown along with the two fitting parameters. The inset shows the behavior at earlier times. Unequal initial decay rates are the result of greater proximity of the γ-crystallites to the paramagnetic-clay surface. No fit is given for the N6C-Is-M-a data because the computation with the same clay−clay spacing (Δ) and the different f_α does not predict the decay. Hence, the conclusion is that well-defined stratification of the γ-phase next to the clay surface does not develop until after annealing. Note that the decay of the NC polarization in the N6C-Is-M-c sample initially lags the decay of the α-crystalline polarization, suggesting that the γ-phase is close to the clay surface.

only if the α-phase crystallites were mostly well-isolated from clay surfaces would the T_1^H of these latter crystallites be notably longer than the average.

We start by illustrating the T_1^H behavior, indirectly detected via the ^{13}C signals, of two N6C-Is-M-c samples that have substantial amounts of both α- and γ-crystallites. These samples had initially been injection-molded at 295 °C and then had been annealed at 214 °C for 18 h. In Figure 1, the 300-MHz T_1^H data are plotted, and in Figure 2, the 100-MHz data for a physically distinct but similar sample are shown. Decays associated with the α- and γ-crystallites as well as the NC protons are distinguished and plotted. Note how the initial slopes for the protons in the γ-crystallites are more rapidly decaying relative to the initial slopes for the protons of the α-crystallites. Note also that the decays of the α- and γ-phase magnetizations are more clearly distinguished at 25 MHz than at 75 MHz. Moreover, after a time of ≈150−200 ms of decay, the slopes of the α- and γ-phase protons become equal, qualitatively indicating that, via spin diffusion, a steady-state polarization gradient has been established on this time scale between these phases. This time frame translates into spin diffusion distances of 15−17 nm (eq 1). Such distances are significantly less than the 40−50-nm average expected separation between clay layers (assuming complete exfoliation) in the N6C-Is-M samples. Thus, we conclude that *the α-rich and γ-rich (semicrystalline) phases are mainly mixed between the clay layers* where the thinnest domain dimensions are likely to be substantially less than the separation between clay layers. In other words, the α-rich phase does *not* arise from isolated regions that have very low concentrations of clay. In addition, from the faster early decay rates of the γ-phase protons, we conclude that *the γ-phase crystallites, rather than their α-phase counterparts, preferentially exist near the nylon/clay interfaces.*

We undertook a simplified calculation that was intended to answer the question whether the shape of the T_1^H decay curves for the α- and γ-crystal magnetizations in Figures 1 and 2 could be mimicked under the assumption of a highly stratified, fully layered morphology, that is, one in which there was a semicrystalline layer containing only the γ-phase in contact with the clay and a similar central sandwiched layer containing only the α-crystallites. The simplified assumptions were as follows: (a) ignore spin diffusion between CR and NC phases (which occurs on a short, 20-ms time scale), (b) the intrinsic T_1^H for both the α- and γ-layers is the spin-diffusion-averaged T_1^H of the dry nylon-6 (i.e., each CR/NC morphology is replaced by a fictitious, uniform phase), (c) clay platelets are parallel to one another and equally spaced, and (d) the paramagnetic influence of the clay on the protons is mimicked by a fast-relaxing but spectrally unobservable, thin (we chose 0.4 nm) layer of nylon, which is in spin-diffusion contact with the rest of the nylon. Via this latter assumption we mainly create a relaxation sink at the surface. The choice of thickness for this fictitious layer is arbitrary and will, especially for very thin layers, dictate the relaxation time, $(T_1^H)_s$, assigned to this region in any fitting procedure. Thus, we will attach only relative and not absolute meaning to $(T_1^H)_s$. Using a diffusion constant, $D = 0.7$ nm^2/ms, we then model both the spin diffusion and the relaxation. The relative thickness of the α- and γ-layers is fixed to be in the same proportion as the α- and γ-crystal fractions. The only parameters varied for the fitting are $(T_1^H)_s$ and the distance, Δ, between the clay surfaces. The data in Figures 1 and 2 represent two samples with approximately comparable f_α values before/after annealing, respectively 0.45/0.75 and 0.33/0.67. We obtained reasonable fits, shown in these figures, for both samples; that is, for the fits shown in Figure 1 at 7.05 T, $(T_1^H)_s = 29.0$ ms and $\Delta = 46.0$ nm whereas for the 2.35 T data in Figure 2, $(T_1^H)_s = 10.8$ ms and $\Delta = 44.8$ nm. So, for these annealed samples, we obtain Δ's that are in good agreement; moreover, these Δ's coincide with the average expected separation (40−50 nm) between platelets for this fully exfoliated sample. If the α- and the γ-crystallites were not strongly stratified, that is, more interleaved, we would expect that the Δ derived from the fit would be unrealistically small relative to the actual Δ.

Another point about Figures 1 and 2 is that, within the signal-to-noise, the magnetization of the γ-phase crystallites begins to decay at a rate close to its maximum rate *immediately following inversion*. There is no lag time during which decay is less than maximum.

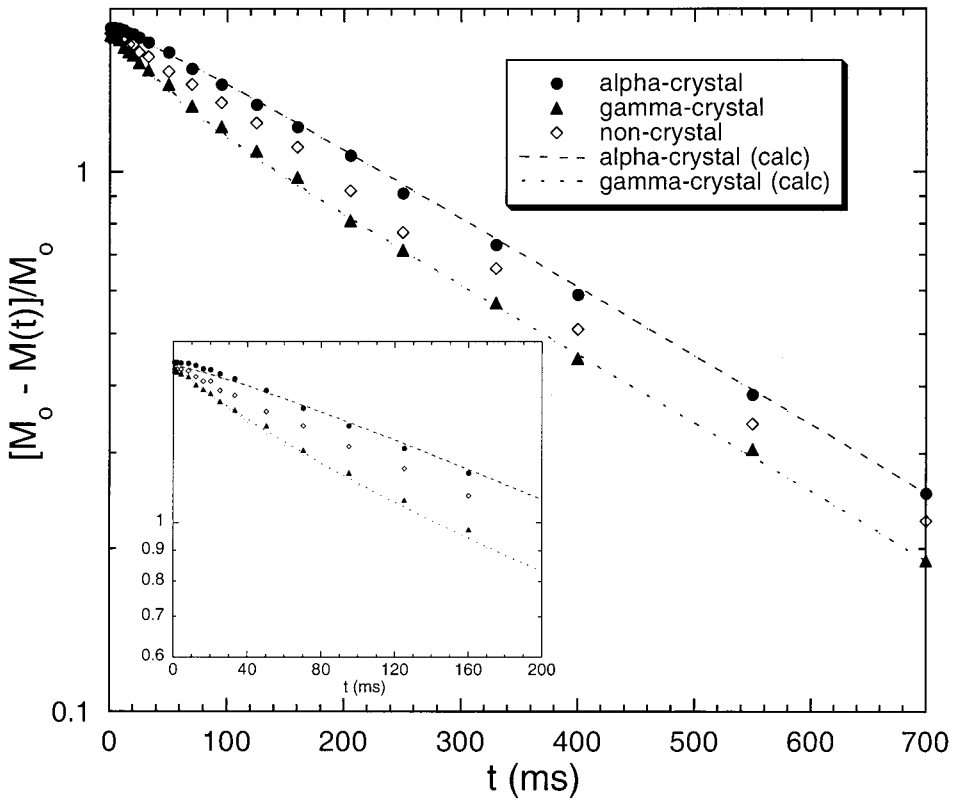

Figure 2. Same as Figure 1 except these are 100-MHz T_1^H data. Only the data and fits for the annealed N6C-Is-M-c sample ($f_\alpha = 0.67$) are shown. The fitted parameters are $(T_1^H)_s = 10.9$ ms and $D = 44.8$ nm ($=2 \times 22.4$ nm). Note the superior separation of the α- versus γ-crystal decays compared to Figure 1. This is almost entirely the result of the (2.7)-fold increase in $(T_1^H)_s$ at 300 MHz. Again, there is little observed contrast (not shown, see text) in the early-time behavior of the α- and γ-crystal proton polarizations prior to annealing when $f_\alpha = 0.33$.

Thus, it is likely that over a significant portion of the clay surface, γ-crystalline domains are in reasonably close contact with the clay surface as opposed to having a thick NC layer separating the clay surface from all the CR regions. This picture would be consistent with (but does not prove) epitaxial crystal growth. Incidentally, the fact that the γ-phase magnetization initially decays faster than the NC magnetization does *not* prove that the γ-phase is in direct contact with the clay surface. The NC chains have, on average, less opportunity to be influenced by paramagnetic relaxation because these chains are not concentrated in a layer near the clay surface as are the γ-crystallites.

Given the above morphological picture of an annealed sample, we can ask whether this highly stratified γ-phase at the clay surface is a general result. We could not, with sufficient accuracy, do the same experiment on samples that had $f_\alpha < 0.15$; this included most of the blended NnC's. The only other sample offering substantial fractions of both crystal phases was the injection-molded sample, N6C-Is-M-a, whose cooling history we do not know very well and whose α-fraction varied from 0.10 to 0.45. We again observed the T_1^H behavior of the magnetizations of the α- and γ-crystals for all samples having $f_\alpha > 0.25$. To our surprise, the result, illustrated only in Figure 1, was obtained for all these samples; that is, there was almost no distinction in the T_1^H decays of both magnetizations. (To be a little more quantitative in this comparison, the ratio, $R_{\alpha/\gamma}$, of the α/γ ordinate amplitudes, for delay times >200 ms, is about 1.14 at 7.05 T and about 1.33 at 2.35 T for the annealed samples in Figures 1 and 2; for the unannealed N6C-Is-M-a sample at 2.35 T, this ratio is in the range 1.05−1.10 and at 7.05 T is <1.05.) We regard $R_{\alpha/\gamma}$ to be a good relative measure of our ability to recognize morphological stratification.

The weak longer-time polarization contrast ($R_{\alpha/\gamma}$ close to unity) in the N6C-Is-M-a sample suggests that the α- and γ-crystallites, following the faster cooling of the injection-molding operation, are not at all well-stratified with respect to the clay surfaces. (We assume here that annealing at 214 °C does not alter, to any significant degree, the relative positions of the clay platelets.) At the same time, recall that f_α increases substantially with annealing. It is expected that, for a fixed Δ, $R_{\alpha/\gamma}$ will increase as the γ-phase becomes thinner in a well-stratified morphology. Thus, if we use the same parameters in our stratified model calculation, changing only the f_α's appropriate to the samples of Figures 1 and 2, then the predicted $R_{\alpha/\gamma}$ values for the annealed (unannealed) samples are 1.33 (1.23) at 2.35 T and 1.13 (1.11) at 7.05 T. The experimental values are significantly less than the values in parentheses; hence, the conclusion stands that the degree of stratification in the injection-molded samples is significantly improved by annealing.

We considered two possible explanations for the poor stratification of the α- and γ-crystallites in the injection-molded samples. The first is that the $R_{\alpha/\gamma}$'s are near unity because the γ-crystallites and the α-crystallites are reasonably well mixed; that is, there is only a slight preference for the γ-crystallites to be located near the clay surface. Perhaps the cooling was rapid enough that nucleation of the α-crystallites in the nylon melt occurred very quickly after the nucleation of the γ-crys-

tallites. (We assume that γ-phase nucleation happens near the clay surfaces, and we also assume, based on DSC studies presented herein, that this γ-phase nucleation occurs at a higher temperature, that is, earlier during cooling, compared with α-phase nucleation.) Then, with the competitive growth of both phases, especially if the α-phase grows faster, the actual spatial distribution of the two types of crystallites would be such that the minority α-phase would not be perfectly "insulated" from the clay layers. A second possible explanation allows for good stratification of the γ-crystallites to regions near the clay surfaces yet also provides weaker-than-expected T_1^H contrast. In the cooling protocol associated with injection molding, the γ-crystallites may be nucleated first by the presence of the clay. These γ-crystallites, therefore, may have a larger crystallite thickness than will the α-crystallites, formed at a lower temperature and a larger undercooling. Thus, the average size of the α-crystallites would be smaller; moreover, they would be less perfect in organization. Smaller size implies closer spin-diffusion contact with the protons in the NC regions and poorer organization allows for more molecular mobility in the CR regions. Both of these latter considerations would tend to shorten $T_1^H$for this α-phase relative to the T_1^H for the γ-phase. Finally, the closer proximity of the γ-phase to the clay surface would then tend to reduce T_1^H preferentially for the γ-phase protons, thereby making the T_1^H's closer, as is observed.

To pursue the possibility of less perfect organization and stronger spin diffusion coupling to NC regions for possibly smaller α-crystallites (second explanation above), we compared the $T_{1\rho}^H$ decay rates for the protons in the α- and γ-crystallites in sample N6C-Is-M-a. Because spin diffusion to protons in NC regions contributes to the effective $T_{1\rho}^H$'s of the CR protons, and because $T_{1\rho}^H$'s for protons in less perfect crystallites should also decrease, we would expect a shorter $T_{1\rho}^H$ for protons in the smaller α-crystallites, relative to the $T_{1\rho}^H$ for protons in the larger γ-crystallites. Within experimental error, both decay rates (not shown) are identical. Hence, there is *no support* for significant size differences between α- and γ-crystallites in this sample.

We illustrate in Figure 3 our best guess as to the morphologies for the unannealed and annealed IsP NnC's where, in the unannealed state, the stratification is poor, mainly because some γ-phase crystallites are not truncated before they approach the middle region between clay surfaces. Crystallites are shown as slightly tapered because there is relatively rapid cooling during growth. Additionally, the γ-phase growth direction in this figure is assumed to be normal to the clay surface, even though, as was previously discussed,[1] not all reported observations agree with this assumption. The α-crystallites nucleate in the central region and do not grow in any preferential direction with respect to the clay surface. In the annealed state, the crystallites thicken slightly while generally maintaining their former position. The thinner regions of the γ-crystallites that are further from the clay surfaces are more susceptible to transformation to the more stable α-form.

In view of the strong paramagnetic perturbations on $T_{1\rho}^H$ that were seen in the OMC's for protons close to the clay surface, it might seem surprising that the γ- and α-phase protons did not show more disparate $T_{1\rho}^H$ behaviors because, on the $T_{1\rho}^H$ time scale, spin diffusion between the CR and NC protons of nylon-6 is expected to be non-negligible. We considered this question and offer the following qualitative explanation. First, over the 20 ms of the $T_{1\rho}^H$ experiment, polarization will only move about 4 nm (use eq 1 with $D = 0.35$ nm^2/ms because D in the rotating frame is half that in the laboratory frame). This means that in a sample where Δ is about 40 nm, 80% of the protons will be outside the range of any influence from the clay paramagnetism. In addition, we looked into the question of whether, using a CP time of 1 ms in our indirect measurements of $T_{1\rho}^H$, we were simply not seeing some signals. To check this, we used a CP time of 0.1 ms and compared samples N6C-B-L1-c (diamagnetic) and N6C-B-M1-c (paramagnetic). We found that the amount of ^{13}C signal lost over the first ms of spin locking was 5−8% larger for the latter sample. Moreover, the line shape corresponding to the lost signal was broad, similar to the NC resonances. Hence, we conclude that there is some additional signal loss associated with the paramagnetism; however, the additional broadening of those resonances near the clay surface interferes with the identification of these resonances as belonging to either the γ- or α-crystallites. The result is that the resonances that are identified as either α- or γ-crystallites are probably at least 2 nm from the clay surface where the direct paramagnetic influences are weak to vanishing.

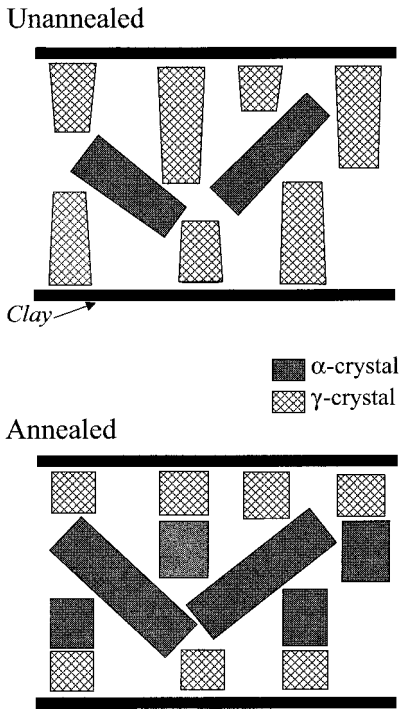

Figure 3. A model for the distribution of the α- and γ-phase crystallites in the injection-molded, in situ polymerized NnC before and after annealing for 18 h at 214 °C. The annealing-induced changes that we attempt to account for are the following: (a) the fraction of α-phase crystallites is assumed to go from about $^1/_3$ to 2/3, (b) the overall crystallinity goes from about 0.33 to 0.41, (c) the stratification of the γ-phase crystallites next to the clay surfaces goes from weak to strong, and (d) at no time during the annealing process is there extensive melting. See text for a discussion of other considerations.

Conditions for Optimizing the Extraction of Morphological Information from the Paramagnetic Nanocomposites. Comparison of Figures 1 and 2 reveal that the stratification of the α- and γ-crystallites between the clay layers is most easily seen in the T_1^H data taken at 2.35 T rather than at 7.05 T. This happens, although the intrinsic $(T_1^H)_{N6}$ for annealed nylon-6 increased about 3-fold from 592 ms at 2.35 T to 1645 ms at 7.05 T, thereby opening up the possibility that the paramagnetic contribution to T_1^H becomes more dominant. The problem is that, according to the fitting parameters, $(T_1^H)_s$ also increases about 3-fold. It turns out that, for a fixed Δ and f_α, $(T_1^H)_s$ determines $R_{\alpha/\gamma}$, so long as $(T_1^H)_{N6}$ is longer than the time for equilibration between the α-rich and γ-rich strata (about 200 ms for the N6C-s-M-c sample). In contrast, $(T_1^H)_{N6}$ determines the *sensitivity* with which $R_{\alpha/\gamma}$ is determined; that is, increasing $(T_1^H)_{N6}$ causes the signals to persist for a longer time so that $R_{\alpha/\gamma}$ can be detected with improved precision. Thus, the attempt to optimize one's ability to extract morphological information from a given sample translates into the effort to find the shortest $(T_1^H)_s$ and the longest $(T_1^H)_{N6}$ ...with a much stronger emphasis on the former condition. If we consider temperature and static field to be the experimental variables, then we know already that higher fields imply longer $(T_1^H)_{N6}$'s and anywhere from a small to a sizable increase in $(T_1^H)_s$. We briefly investigated the influence of temperature on these parameters at 7.05 T and found that, for the N6C-B-M1-b sample over the range from 260 to 340 K, T_{1para}^H and $(T_1^H)_s$ are essentially independent of temperature (consistent with the idea that electron spin exchange, rather than the intrinsic T_1^e, determines the spectral density for relaxing the nearby nuclei). On the other hand, we also measured the T_1^H of N6. Relative to $(T_1^H)_{N6}$ at 300 K, there is a 50% increase at 260 K and a 40% decrease at 340 K. So one can achieve a modest, desirable increase in $(T_1^H)_{N6}$ by lowering the temperature. Thus, we conclude that lower fields and lower temperatures favor the extraction of morphological information unless one is confident that the relevant spectral densities have only a weak field dependence. In the latter case, higher fields and lower temperatures would offer improved sensitivity.

In summary, the most important variable for optimizing the conditions for detecting morphological stratification at clay surfaces is the Fe^{3+} concentration in the clay. Finding that Fe^{3+} concentration which maximizes the spin-exchange-determined spectral density at the experimental Larmor frequency of the protons is the best way to optimize ones ability to detect stratification. We have just begun to investigate the influence on T_1^H of montmorillonite clays with different Fe^{3+} contents. Preliminary results suggest that the clay used in the nanocomposites from Southern Clay Products has a near-optimum Fe^{3+} content (reported by Doug Hunter of Southern Clay Products to be 4.2 mass % Fe_2O_3 for the crude Na^+−montmorillonite clay). However, at this point, that conclusion is not firm. In fact, we will not discuss those data more because we lack independent information as to whether the clay dispersions are similar in all samples and whether the Fe^{3+} ions are all found in comparable chemical sites in the clays.

Regarding the Chemical Stability of the Organic Modifier during Processing. One of the roles of the OM is to facilitate the mixing of the nylon-6 and the clay. It does this, presumably, by initially increasing the spacing between clay layers, thereby weakening the electrostatic interactions between clay layers. Also, one would like to select an OM that will generate thermodynamic affinity between the polymer and the OM. Eventually, after the composite is formed, the OM should also play some role in mechanical properties by helping to define the mechanical coupling between the polymer and the reinforcing clay platelets. We were, therefore, interested in the fate of the OM under processing conditions. What we present here is preliminary and pertains mainly to the suite of N6C-B-M3 samples where processing parameters were varied in the blending of a given formulation of the nanocomposite. While the ambient-temperature proton methods employed in the analysis of this suite of samples offers reasonably clear, albeit somewhat unexpected results, we are not in a position to claim that this methodology will be equally effective in following chemical degradation for other OM's.

The OM, used for the N6C-B-M3 samples, is a tetrasubstituted ammonium ion containing two hydrogenated-tallow substituents and two methyls; designate this ion "M_2T_2AI". Even though the montmorillonite clay used in this formulation can be neutralized, in terms of its average charge density, by reaction with $(M_2T_2AI)^+Cl^-$ at 0.95 equiv/kg of clay, 1.25 equiv were actually used to "improve" the mixing behavior with nylon-6. (Some OM's do not require this excess application.) Thus, about one-fourth of the applied OM might still be present with its Cl^- anion. The fact that the clay spacing is found to be about 3.1 nm in this OMC, compared to 1.8 nm in the OMC used in the "M1" samples of Table 1, suggests that the excess OM is truly between the clay layers.

Typically, in the NnC's that we studied, the OM associated with the clay would constitute a mass fraction of about 2−3% of the total organic content of the NnC. For the OM molecules that are attached to montmorillonite clay surfaces, the paramagnetic character of this clay creates significant spectral broadening and makes chemical-shift identification of the protons (or carbons) difficult.[1] Thus, we were surprised to see, on top of the broad line shape of the nylon-6 in the Bloch-decay spectra of the dried N6C-B-M3 samples, *narrow* proton resonances, whose intensities, relative to the total intensities, were in the 1−3% range. By comparison, such narrow resonances were <0.03% in the spectra of the pure nylon-6. Thus, there is no possibility that water or some additive in the nylon-6 could give rise to these more intense narrow lines in the NnC's. In Figure 4 we show full Bloch-decay spectra as well as expanded "centerband" spectra of the narrow component for the three N6C-B-M3 samples plus the N6C-B-M1-b sample at $\nu_r = 5$ kHz. Also shown for reference is the Bloch-decay spectrum of nylon-6 (note that for $\nu_r = 5$ kHz one sees a small sideband pattern but that the width of the spinning sidebands is much broader than that for the narrow resonances being discussed here). Finally, we also show the narrow resonances for the *original pellets* for the N6C-B-M3-c sample, prior to the high-temperature exposures in-

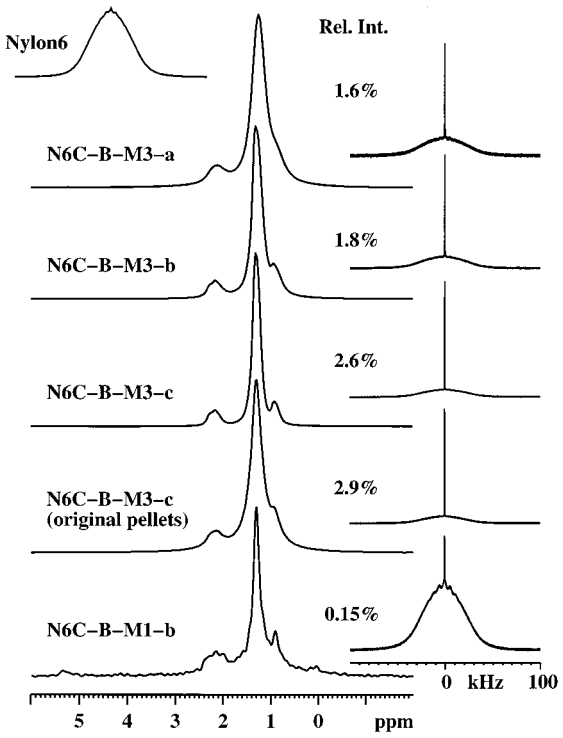

Figure 4. 300-MHz proton spectra (ν_r = 5 kHz) of nylon-6 and the indicated NnC's showing the spectral signatures of the chemically degraded, phase-separated, mobile organic modifier (OM). Spectra on the right and upper left are full Bloch-decay spectra, normalized to the same peak height. The very narrowest corresponding centerband resonances are shown on the left, except for nylon-6 which has no such narrow resonances. These have been separated quantitatively from the broad component using an echo sequence (see text). Narrow-component intensities, relative to the total NnC intensities, are also given. Resolution and relative intensities within each narrow component allow us to identify chemically the main degradation product. These data also allow us to comment on the processing conditions that lead to degradation and on the relative stability of different OM's (see text).

volved in the SC process. In each case, the narrow resonances have been extracted via a (90°−τ−180°−τ−observe) echo sequence[19] with τ = 200 ms = 1 rotor period. The mobility of the molecules giving rise to these narrow spectral features is high enough so that this echo sequence preserves >96% of the narrow component present in the Bloch-decay spectra. At the same time, the echo spectra eliminate the nylon-6 contributions, including the contribution from the broader spinning sidebands.

The relative intensities of the narrow components, relative to the integral of the entire NnC proton signal, are collected in Table 4. One of the most important conclusions from the data of Table 4 (and illustrated for the N6C-B-M3-c sample in Figure 4) is that the amount of the narrow component does not change during the preparation of the SC materials. The only change was that the resonances of the narrow component sharpened a bit after the SC treatment. The three N6C-B-M3 samples represent substantial variations in the intensities of the narrow component. Moreover, the processing steps in the subsequent SC protocol exposed the samples to equivalently high temperatures and for much longer times than these samples had experienced upon blending. Yet, it evidently was the *combination of temperature and the mechanical stresses of blending, rather than just temperature itself, that was the principal cause of the chemical degradation of this OM*. The high mobility of these degraded OM molecules most probably indicates a phase separation of this mobile component within the polymer matrix. We speculate that the sharpening of the lines for the narrow component of the SC samples represents a growth or ripening of the domain size for this narrow component and a corresponding lessening of the influence of the polymer domain walls on the motion of these smaller molecules.

Table 4. Relative Proton Intensities, Referenced to the Total Proton Integral, of the Narrow Spectral Component for Selected Samples in the Form of the Original Pellets or after the Pellets Had Been Melted and Slowly Cooled (SC)[a]

nanocomposite	intensity (SC) (%)	intensity (original pellets) (%)	f_d[b]
N6C-B-M1-b	<0.15(3)	<0.08(2)	0.06(3)
N6C-B-L1-b	0.22(3)	0.18(3)	0.09(3)
N6C-B-M3-a	1.6(2)	1.4(2)	0.43(8)
N6C-B-M3-b	1.8(2)	1.8(2)	0.51(6)
N6C-B-M3-c	2.6(3)	2.9(3)	0.79(13)
N6-a (nylon-6)	<0.03	<0.03	N/A

[a] Standard uncertainties, in units of the last significant figure, are given in parentheses. The fraction, f_d, of the original OM that has decomposed to form this narrow component is also given. [b] This fraction of decomposed OM molecules is based on the following information and assumptions: (a) the weight fraction of the OMCs that is lost up to a temperature of 900 °C in a TGA determination, (b) a 5% loading of the OMC in the NnC, (c) every ion of the OM that decomposes produces at least one nonvolatile molecule that subsequently phase separates into a region with near isotropic motions, (d) every decomposed (M_2T_2AI) ion of the OM in the N6C-B-M3 samples produces one MT_2N molecule and every decomposed [$MT(HE)_2AI$] ion produces one (MTXN) molecule where X is not specified other than that it is not tallow (T). Thus, the number of decomposed ions can be related to the 0.9 and 1.3 ppm intensities of the tallow ("T") substituent for the N6C-B-M1-b and N6C-B-L1-b samples.

In Table 4 we have also included data for samples N6C-B-M1 and N6C-B-L1. These samples have an OM that is a more polar (see Table 1) tetrasubstituted ammonium ion. In Figure 4 the narrow component for sample N6C-B-M1 has an amplitude that is about an order of magnitude smaller than that in the N6C-B-M3 samples; however, its chemical shift profile is similar with the exception that the resonance near 2.2 ppm is significantly broader and relatively more intense.

We note a few things about the spectra of Figure 4. First, in the full spectra, there are no spinning sidebands that have the narrow signature of the narrow centerbands. Hence, these molecules are rapidly and nearly isotropically tumbling. In fact, in spectra of nonspinning samples (not shown), these narrow resonances are easily identified, although there is little chemical shift resolution. The narrowness of the lines implies that the corresponding molecules are probably more than 2 nm from the surface of the clay; if they were closer, their proton resonances would be broader, especially in the nonspinning mode, and such magnetization would not easily survive the echo sequence. Second, the relative intensities vary considerably; this is especially notable in the N6C-B-M3 samples. The fact that these samples have the same formulation makes it especially unlikely that the narrow component rep-

(19) Hahn, E. L. *Phys. Rev.* **1950**, *80*, 580.

resents some common impurity. (Also, these are very well dried samples, so we are not looking at water molecules dispersed in the nylon.) Third, the chemical shifts that can be resolved in the N6C-B-M3 spectra tend to cluster near the shift values of 0.9, 1.3, and 2.2 ppm. The first two shifts are those of methyl and methylene protons on aliphatic chains (i.e., the hydrogenated tallow) in the liquid state[20] and the 2.2 ppm peak is typical[20] of liquid-state protons attached to carbons that are bonded to an **amine** nitrogen (not an ammonium nitrogen whose shifts would lie just above 3 ppm...an empty region in our spectra). Moreover, the 2.2 ppm intensity is about 10% of the total intensity for each of the narrow-component N6C-B-M3 spectra in Figure 4. On the basis of this latter information and on the chemical shift assignment, we identify the narrow component in the three N6C-B-M3 samples as MT_2N, a tertiary amine with one methyl and two hydrogenated tallow substituents. If the decomposition of the M_2T_2-AI had produced mainly M_2TN, then the 2.2 ppm peaks would have been almost twice as intense. The spectrum of the narrow component of the N6C-B-M1 sample shows evidence of the tallow substituent (0.9 and 1.3 ppm); however, the 2.2 ppm region is quite broad and represents about 22% of the total intensity of the narrow component. While we are tempted to interpret this spectrum as representing an amine with a single tallow substituent, we are less sure of the other two substituents. Probably one is a methyl, but the lack of resonance intensity in the region from 2.5 to 5.5 ppm makes us skeptical whether any hydroxyethyl substituents are present.

The significantly lower intensity associated with the narrow component of the N6C-B-M1-b sample compared to the N6C-B-M3-a,b samples suggests that the *$MT(HE)_2AI$ is a more stable OM than the less polar M_2T_2AI*. From Table 1, the N6C-B-M1-b sample has the second shortest T_1^H of this group; hence, it has the second best clay dispersion of this group, thereby offering more exposed surface and more opportunity for decomposition of the OM than was true for the N6C-B-M3-(a,b) samples. But the resistance to decomposition was evidently about an order of magnitude higher albeit some of this added stability might, in principle, derive from more favorable blending conditions; we have been unable to trace the conditions. We note that this greater OM stability is also supported by the fact that a smaller molar amount of $MT(HE)_2AI$ is required for producing good mixing than for M_2T_2AI. At the same time, one should recognize that the above arguments depend on the unproven assertions that all of the major decomposition products phase separate into regions of high molecular mobility and that these products are also minimally volatile at 240 °C. In this connection, none of the IsP NnC's showed any significant narrow component. Whether this indicates higher stability of the OM (owing to its presumed covalent incorporation into the polymer) or higher volatility of the decomposition products...or a lack of phase separation is not known. However, the large contrast in f_α (Table 1) between the recrystallized and annealed N6C-Is-M-e and N6C-Is-M-h samples (the former having seen a peak temperature of 295 °C and the latter, 250 °C) may still relate to some modification of the clay surface involving some decomposition of the OM. The lower crystallization temperature for the melted N6C-Is-M-c sample[1] compared to the melted N6C-Is-M-h sample, can imply, along with the possibility of a diminished molecular mass, that some chains in the former sample are no longer tethered to the clay surfaces.

(20) *Aldrich Library of ^{13}C and ^{1}H FTNMR Spectra*; Pouch, C. J., Behnke, J., Eds.; Aldrich Chemical Co., 1993.

Discussion

Considering that clay promotes the growth of the γ-phase, we were surprised that γ-crystallites in the IsP injection-molded sample have only a weak average preferential proximity to the clay surfaces relative to the α-crystallites that are present. At the same time, after annealing at 214 °C, there is both a substantial increase in the fraction of α-crystallites *and* a distinct preferential proximity of the γ-phase crystallites to the clay surface. Moreover, using a model in which there is complete stratification of the γ-rich and the α-rich regions, one obtains decent fits to the T_1^H data and reasonable values for the separation between clay platelets. (Obtaining a reasonable separation supports the notion that stratification is very well defined after annealing.) How does the system go from little to almost complete α/γ stratification upon annealing? Did the system fully melt at some point during annealing? This possibility can be dismissed because the DSC results[1] for sample N6C-Is-M-c, contrasted with its N6C-Is-M-d counterpart, indicate that, at the end of the annealing period, most of the crystallites had formed (yielding high-temperature melting peaks) before cooling begins; so one would suppose that a minimal amount of molten nylon-6 is present at any time during annealing. The only clue that we have about the nature of the annealing process for the injection-molded samples is that there is some correlation between the f_α values before and after annealing. Because, on the basis of the T_1^H data, the variation in the initial f_α values is not a result of substantial differences in the dispersion of clay...but more likely due to local differences in cooling rates, it is likely that those regions with the highest f_α values have cooled the fastest; hence, they would also have the thinnest crystallites. Because we assume that growth of the γ-crystallites is initiated at or near the surface of the clay, the tendency would be that during relatively rapid cooling these crystallites would become thinner (in the chain-axis direction) as they grew. Thus, the thinnest regions would probably be furthest from the clay surface, assuming growth in a direction normal to the clay surface. The thinnest regions of the crystallites would thus be more subject to reorganization, including melting and recrystallization, during annealing. If we further assumed that anything that melted during annealing would convert to the α-form, especially if there were some α-crystallites already present that could serve as growth templates, then one might begin to rationalize why the injection-molded, annealed N6C-Is-M samples developed stratification of the γ- and α-crystallites relative to the clay surfaces. A transformation from γ to α of mainly the thinner crystallites, possibly but not necessarily via melting and recrystallization, would also be consistent with observations that the SC samples, which had ample time to form thicker

γ-crystallites, would have γ-crystallites that were much more stable to annealing at 214 °C. The one exception (discussed in the next paragraph) to this "stability" of the SC samples is the pair, N6C-Is-M-(d,e), where a large conversion from γ to α was observed upon annealing. We emphasize, however, that the foregoing speculations do not entirely dismiss the possibility that there is something about the polymer/clay interactions that can also, at annealing temperatures, stabilize those γ-crystallites, which are in close proximity to the clay surfaces. Perhaps the more limited entropy gain upon melting of those nylon-6 segments that strongly interact with the clay surface has the effect of increasing the melting point of the nearby adjacent crystalline stems. In this way, the γ-crystallite regions close to the clay surface might be preserved in the γ-phase.

With respect to measuring the relative quality of clay dispersion, one could imagine that the α/γ ratio of crystallites might, under tightly controlled circumstances, be used as a relative measure of clay dispersion. In view of the fact that the rate of cooling has a lot to do with the appearance of the α-phase at the nominal 5% loadings used herein, one would suppose that if the α/γ ratio were to be useful in this sense, that one would have to go to rather thin films and rapid cooling rates, that is, significantly faster than the air cooling of extruded pellets, and that the cooling rates ought to be very reproducible. We viewed such a possible protocol as unwieldy and, therefore, pursued the idea that T_1^H would give us this information. However, in order for T_1^H to be used as a relative measure of clay dispersion, one needs a paramagnetic clay, for example, a montmorillonite with embedded Fe^{3+} ions, and one also needs to hold several parameters constant. These parameters are as follows: (a) type of clay and its Fe^{3+} concentration, (b) polymer/clay stoichiometry, (c) temperature and B_o value of measurement, (d) level of nylon-6 hydration (preferably dry), and (e) crystallization history.

In terms of the sensitivity that T_1^H will have to the quality of clay dispersion, given a particular nylon/clay stoichiometry, the most critical thing is to obtain a clay with optimum spectral density for producing proton relaxation at the Larmor frequency of the protons. Because there are strong indications that the spectral density of magnetic fluctuations near montmorillonite clay surfaces originates mainly from spin-exchange interactions between electrons on neighboring Fe^{3+} sites, one expects the spectral density to be determined mainly by the Fe^{3+} concentration, as opposed to some intrinsic T_1^e. Of the two paramagnetic clays used in this study, the clay used for the blended NnC's is superior in this regard to the clay used for the in situ polymerized NnC's. (See Table 3.) Qualitatively, because T_{1para}^H, isolated from T_1^H via eq 2, is the parameter sensitive to the quality of clay dispersion, one can isolate T_{1para}^H with more accuracy when $(T_1^H)_{N6}$ for pure nylon-6 is the longest, relative to T_{1para}^H. We have observed herein that $(T_1^H)_{N6}$ increases with increasing B_o and with decreasing temperature. We have also observed that T_{1para}^H for a given sample is not very sensitive to temperature (at least over a limited range of ±40 °C); however, its sensitivity to B_o varies. T_{1para}^H will either increase or remain about constant with increasing B_o, the latter being the preferable situation. If, for example, one has a montmorillonite like that used in the blended NnC's, whose T_{1para}^H is only slightly smaller at 7.05 T relative to 2.35 T, then the best conditions, of those we explored, for accurate determination of the quality of clay dispersion were those at 7.05 T and 260 K. Note that we really have explored only two montmorillonite clays in this study. We are in no way claiming that the clay used in the blended NnC's is the optimum clay to use. It is conceivable that other clays with higher Fe^{3+} concentrations will be superior. At some point, the Fe^{3+} concentration will become sufficiently high and the fluctuations sufficiently fast so that the spectral density at the Larmor frequency will begin to diminish. While we cannot say with certainty what the optimum concentration is, we do not expect major increases in the efficiency of induced relaxation, over that seen in the clay used for the blended NnC's. This claim is based on the flatness of the spectral density between 100 and 300 MHz, the latter indicating that fluctuations are very close to, if not exceeding, the Larmor frequency in these materials. Also, given the statistical distribution of Fe−Fe distances in the clay layers, one expects the distribution of spectral densities associated with electron spin fluctuations to be quite broad, as is borne out by the observation that the $T_{1\rho}^H$ (as well as the T_1^H) is shortened by about 2 orders of magnitude for the protons in the OMC's. Broad distributions yield more slowly changing spectral densities.

One can also ask the question of how sensitive T_1^H or T_{1para}^H is to the quality of clay dispersion. First, because these are single parameters, they will not be very sensitive to inhomogeneities in the dispersion. One should rather expect to deduce information about the average distance, Δ, between clay layers. Consider, then, how Δ and T_{1para}^H, or the clay concentration, C, and T_{1para}^H might be related. Because we have not been able to generate a closed-form relationship between these quantities, we will address this issue on the basis of the results of modeling calculations of the sort described earlier and illustrated in the fits to the data of Figures 1 and 2. Suppose that a given T_{1para}^H corresponds to a given Δ. Then, if ϵ_p is defined to be a small fractional change in T_{1para}^H ($\epsilon_p = \delta T_{1para}^H / T_{1para}^H$), we want to estimate the corresponding fractional change, η ($=\delta\Delta/\Delta$), in the quantity Δ. For the range, $45 < \Delta < 100$ nm, which pretty well covers the region of interest in these samples, it is a good approximation that ($T_{1para}^H \propto \Delta^\beta$), where β is a function of $(T_1^H)_s$, the relaxation time assigned, in our model calculation, to the thin (0.4 nm) layer next to the clay surface. The quantity, β, ranges from 1, in the limit where $(T_1^H)_s > 75$ ms, to about 2, when $(T_1^H)_s < 0.5$ ms. These two regions correspond to the "relaxation-controlled" and the "diffusion-controlled" regimes, respectively. For the IsP samples, β is about 1.3 for the 2.35 T data (Figure 2) and is about 1.1 for the 7.05 T data (Figure 1). Our best guess for β in the blended NnC's is about 1.5, considering the fact that, compared to the IsP sample, the density of clay layers is lower and $(T_1^H)_s$ should be shorter, owing to the higher density of Fe^{3+}. From the above, $1.5\eta > \epsilon_p > 1.1\eta$ for our samples. If the quality of the clay dispersion is expressed as a concentration, C, of effective clay particles, then one must relate C to Δ. In the limit of higher C where clay layers are highly parallel, $\Delta \propto C^{-1}$. At

infinite dilution, $\Delta \propto C^{-1/3}$. For these samples where the average separation between layers in a well-exfoliated sample is of the same order as the lateral dimension of each clay layer, there is an intermediate amount of parallel ordering of the clay. So, for this exercise, we assume an intermediate value, that is, $\Delta \propto C^{-0.6}$. Finally, we measure changes in $T_1{}^H$, not in $T_{1para}{}^H$. Hence, if ϵ_o is defined as the fractional change in $T_1{}^H$ and η_c is the corresponding fractional change in clay concentration, then $\epsilon_o \approx (T_1{}^H/T_{1para}{}^H)\epsilon_p \approx (T_1{}^H/T_{1para}{}^H)\beta\eta \approx 0.6(T_1{}^H/T_{1para}{}^H)\beta\eta_c$. If we assume $\beta = 1.3$ and $(T_1{}^H/T_{1para}{}^H)$ takes on a typical value (see data in Tables 1 and 3) of $^1/_3$, then $\epsilon_o \approx 0.26\ \eta_c$. The foregoing implies that if we can measure $T_1{}^H$ to a precision of ±2.5%, then we can expect to pick up changes in clay concentration above the ±10% level. Picking up changes at this level ought to be adequate for process monitoring or for assays of the extent of exfoliation in the presence of different OMs. The foregoing is a crude estimate. Obviously, one of the significant parameters for improving sensitivity to fluctuations in C is to increase $(T_1{}^H/T_{1para}{}^H)$. That is an important reason for finding a clay with optimal Fe^{3+} concentration.

As to the OMs and their stability in processing, the OM whose decomposition we monitored is one that represents a class of substituted ammonium cations. Hence, its chemistry of decomposition to free amine probably has generality, even though it is not necessarily the best performing OM. Compared, for example, to the $MT(HE)_2AI$ used for the N6C-B-M1 samples, M_2T_2AI might be argued to be an inferior OM because it required a 30% molar excess to produce good blending whereas the $MT(HE)_2AI$ is used at near-stoichiometric amounts. In fact, in the OMCs, the spacings determined from X-ray diffraction are 1.85 nm ($MT(HE)_2AI$) and 3.15 nm (M_2T_2AI) with corresponding gallery widths of about 0.85 and 2.15 nm. Thus, the bulkier character (two tallow substituents rather than one) of the M_2T_2AI coupled with the 30% excess, results in more than a doubling of the gallery width. One might presume that the greater separation between clay layers in the OMC containing M_2T_2AI would better promote exfoliation. Perhaps this is so; however, in the presence of shear-induced exfoliation, this OM seems to have more affinity for itself than for the nylon-6. Perhaps this increased self-affinity is a consequence of the two tallow substituents. Hence, the decomposed OM appears to be wiped off the surface as the free amine, (MT_2A), no doubt leaving behind some ionic species at the surface of the clay for charge neutralization. It is interesting that even though the 30% excess material initially has a neutralizing anion present, probably Cl^-, that there is no evidence of any phase-separated ammonium species present after decomposition, this although the decomposed material in the N6C-B-M3-c sample (Table 4) probably originated, in part, but certainly not entirely, from the "excess" OM. We note in passing that the concentration of chloride ion in the OMCs prior to blending is certainly higher in the N6C-B-M3 samples relative to the N6C-B-M1 sample. A point to consider is the possibility that the presence of this ion somehow promotes degradation of the OM to the free amine.

While the detected decomposition of the $MT(HE)_2AI$ is not nearly as extensive as that for the M_2T_2AI, the material that is detected is again identified to be free amines, albeit the extra intensity in the 2.2 ppm region has not been assigned to specific substituents. The weak resonance in the 5.1−5.3 ppm range could, in principle, be hydroxyl or residual unsaturation in the tallow chains. Nevertheless, the weakness of the peak makes it doubtful whether the hydroxyethyl moiety has stayed intact as a substituent. It is important to remember that the greater stability of the $MT(HE)_2AI$ compared to the M_2T_2AI is not the only explanation for the observation of a weak narrow component. Other explanations might include (a) higher volatility of the product or (b) higher solubility in the nylon-6 matrix and more restricted motion (broader, unresolved lines).

The finding that chemical degradation of the M_2T_2AI is mainly due to the **combination** of temperature and shear forces in blending, rather than simply due to temperature, underscores the need for strong binding of the OM to the surface to retain the OM in a blending operation. However, the fact that good mixing could still be accomplished in the N6C-B-M3-c sample, despite the extensive decomposition, raises the question of whether the OM, besides facilitating the initial separation of the clay layers, plays an important role in establishing the mechanical properties of the material. Whether the mechanical properties depend on good strong interactions between the clay surface and the nylon-6 remains an open question, so far as this study is concerned.

Conclusions

The use of paramagnetic montmorillonite clays for NnC formulations was seen as an opportunity to deduce useful information. First, we were able to use the overall $T_1{}^H$ of the nylon-6 protons as a relative measure of the quality of clay dispersion within families of NnC's formulated with the same clay, the same nylon/clay stoichiometry, the same state of dryness, and the same thermal history. Second, because the paramagnetic influence on $T_1{}^H$ is by spin diffusion from the clay surface, the effective $T_1{}^H$ of those regions closer to the clay surface is shorter than for those regions further away. Hence, we have a ^{13}C NMR morphological tool for investigating the stratification of morphology with respect to the clay surfaces, starting at distances of ≈2 nm from the clay surfaces. In the case of the IsP injection-molded samples, where the fractions of α- and γ-crystallites were both non-negligible, it was found that, surprisingly, the average proximity of the γ-phase crystallites to the clay surface was hardly greater than that for the α-phase. However, upon annealing, there was extensive stratification along with a substantial increase in the fraction of crystallites of the α-form. Among other conclusions, this observation reinforced the notion that the clay surface has, in this case, a capacity to stabilize nearby γ-crystallites, even under annealing conditions, to distances on the order of 8 nm from the clay surface. Also, the use of two different montmorillonite clays with different levels of Fe^{3+} and the collection of data at two different magnetic fields helped to establish the mechanism of electron−electron spin exchange as the important mechanism that determines the influence of the paramagnetism on the proton relaxation times. This recognition leads to the notion that there is an optimum concentration of Fe^{3+} in the

clays that allows one to perform the above two experiments most efficiently.

Finally, we observed proton spectra of the decomposition product of the organic modifier (OM), dimethyl, dihydrogenated-tallow ammonium ion. Upon blending this organically modified clay (OMC) with nylon-6 at 240 °C, most of the nylon-exposed clay layers suffered degradation of this OM, thereby forming phase-separated mobile domains of methyl, dihyrogenated-tallow amine. Subsequent melting at 240 °C resulted in no significant further production of this amine. Degradation studies led to three conclusions: (a) the foregoing OM is probably much less stable than are, say, methyl, tallow, bis-2-hydroxyethylammonium ion or 12-aminolauric acid (the OM used in the in situ polymerized NnC's). (b) It is a *combination* of shear stress and temperature, rather than temperature alone, that produces the extensive OM degradation observed. (c) Having an intact OM is not a necessary condition for achieving good mixing.

We are currently investigating the optimization of the Fe^{3+} concentration for elucidating morphology. We are also pursuing the degradation of molecular mass upon high-temperature injection molding for the in situ polymerized samples.

Acknowledgment. We thank Dr. Doug Hunter of Southern Clay Products for samples and for providing other characterization data for the nanocomposites. We also thank Dr. Alexander Morgan for assistance with TGA and elemental analyses.

CM011078X